Structure of ^{112}In nucleus

T. Kibédi, Zs. Dombrádi, T. Fényes, A. Krasznahorkay, J. Timár, and Z. Gácsi
Institute of Nuclear Research of the Hungarian Academy of Sciences, H-4001 Debrecen, Hungary

A. Passoja*
University of Jyväskylä, Department of Physics, SF-40100 Jyväskylä 10, Finland

V. Paar and D. Vretenar
Prirodoslovno-Matematički Fakultet, University of Zagreb, 41000 Zagreb, Yugoslavia
(Received 12 January 1988)

The γ-ray spectra of the ^{112}Cd(p,nγ)^{112}In and ^{109}Ag(α,nγ)^{112}In reactions were measured with Ge(Li) spectrometers for bombarding energies of 4.8 MeV protons and 17.1 MeV α particles. The energies and relative intensities of 79 ^{112}In γ-ray transitions have been determined. The electron spectra were measured with combined magnet plus Si(Li) as well as superconducting magnetic lens plus Si(Li) spectrometers. Internal conversion coefficients of 40 ^{112}In transitions have been determined, and the level scheme of ^{112}In, γ-ray branching ratios and transition multipolarities have been deduced. Computed Hauser-Feshbach (p,n) cross sections were compared with experimental ones, obtained from γ-ray measurements. On the basis of the internal conversion coefficients and Hauser-Feshbach analysis, level spins and parities have been determined. The energies of several ^{112}In proton-neutron multiplets were calculated on the basis of the parabolic rule derived from the cluster-vibration model. The level energy spectrum and electromagnetic properties were calculated on the basis of the interacting boson-fermion-fermion/odd-odd truncated quadrupole phonon model and satisfactory agreement was obtained between the experimental and theoretical results. More than 20 p-n multiplet states have been identified in ^{112}In.

I. INTRODUCTION

The excited states of the ^{112}In nucleus have been investigated by Hjorth and Allen[1] from (d,t) reactions, by Brinckmann *et al.*[2] and Fromm *et al.*[3] from (α,npγ) and (d,2nγ), by Eibert *et al.*[4] from (α,nγ) and (^{6}Li,4nγ), by Samuelson *et al.*[5] from (α,d), by Emigh *et al.*[6,7] from (^{3}He,d), (p,d), (α,nγ) and (p,nγ), and by Adachi *et al.*[8] and Kohno *et al.*[9] from (p,nγ) reactions. Valuable information was obtained on the energies, spins, parities, and γ decay of excited levels, on $\gamma\gamma$ coincidences, the angular momentum of the transferred nucleon, spectroscopic factors, etc.

The experimental nuclear structure data available were compiled by Peker.[10] The internal transitions from the 156.61 keV $J^\pi=4^+$ (20.9 min) and 613.82 keV $(8)^-$ (2.81 μs) isomeric states were investigated also in several works.[11–18]

On the other hand, internal conversion coefficients (ICC) have been measured only for three transitions[3,11] (from isomeric states) and the level spins and parities are missing or ambiguous in many cases.

Theoretical results on the structure of ^{112}In have been obtained primarily on the $\pi\tilde{g}_{9/2},\nu\tilde{h}_{11/2}$ multiplet and two positive parity states. Eibert *et al.*[4] have calculated the energies of the $\pi\tilde{g}_{9/2},\nu\tilde{h}_{11/2}$ multiplet members using a long-range multipole interaction. Van Maldeghem *et al.*[19] performed calculations within the framework of neutron-quasiparticle proton-hole coupled to quadrupole phonon excitations of the underlying core.

The aim of the present work was the measurement of the γ-ray and conversion electron spectra of the ^{112}Cd(p,nγ)^{112}In and ^{109}Ag(α,nγ)^{112}In reactions, determination of the multipolarities of the ^{112}In transitions, deduction of spin and parity of levels (from the internal conversion coefficients and the Hauser-Feshbach analysis), the calculation of the energy splitting of several positive and negative parity p-n multiplets on the basis of the parabolic rule derived from the cluster-vibration model, the identification of p-n multiplet states, and the calculation of the energy spectrum and electromagnetic properties of ^{112}In in the interacting boson–fermion-fermion/truncated quadrupole phonon model for odd-odd nuclei (IBFFM/OTQM).

II. EXPERIMENTAL TECHNIQUES

A. (p,nγ) reaction

An isotopically enriched, rolled, self-supporting 1.6 mg/cm^2 thick ^{112}Cd target was used in the measurements. For the reliable identification of γ rays we have studied also the ^{113}Cd + p and ^{114}Cd + p reactions with γ-spectroscopic methods, using enriched targets. The isotopic composition of the targets and the corresponding (p,n) reaction Q values are given in Table I.

The targets were bombarded with $E_p=4.8$ MeV energy and $I_p=5-500$ nA intensity proton beams of the

TABLE I. Isotopic composition of the enriched Cd targets (in %)[a] and the Q energy values of the ^{A}Cd(p,n)^{A}In reactions.

Target \ Isotope	^{106}Cd	^{108}Cd	^{110}Cd	^{111}Cd	^{112}Cd	^{113}Cd	^{114}Cd	^{116}Cd
^{112}Cd		0.05	0.24	2.01	95.5	1.34	0.71	0.05
^{113}Cd	<0.1	0.14	0.48	0.29	0.67	95.5	2.68	0.24
^{114}Cd			0.6	0.6	1.24	1.43	94.9	1.27
Q(p,n) (MeV) (Ref. 21)	-7.33	-5.91	-4.72	-1.65	-3.37	-0.47	-2.23	-1.26

[a]According to the certificate of Techsnabexport (Moscow).

Jyväskylä 90-cm cyclotron. The γ-ray spectra were measured with 62 and 82 cm^3 Ge(Li) detectors, which had ~ 1.7 keV energy resolution at 1332 keV. For the energy and efficiency calibration of the γ spectrometers we used ^{133}Ba and ^{152}Eu sources. The energies of several strong ^{112}In lines were already known from the measurements of Kohno *et al.*[9] These energies were confirmed by our measurements within an uncertainty of 50 eV. The γ-ray spectra were measured at $\theta \sim 125°$ angle to the bombarding beam direction.

For conversion electron measurements a combined intermediate-image plus Si(Li) spectrometer[22] was used. The energy resolution and the detection solid angle of the spectrometer were ~ 2.5 keV (at 976 keV) and $\sim 10\%$ (of 4π), respectively. The emission angle of electrons leaving the target and detected by the Si(Li) detector was about 40°. For energy and efficiency calibration of the electron spectrometer we used an ^{152}Eu source.

B. (α,nγ) reaction

Self-supporting targets, $\simeq 0.8$ and $\simeq 0.4$ mg/cm^2 thick, were prepared for γ- and e$^-$-spectrum measurements from isotopically enriched (to 99%) ^{109}Ag by the evaporation technique. For the reliable identification of γ rays we have studied also the ^{107}Ag$+\alpha$ reaction using an enriched (to 99%) ^{107}Ag target.

The targets were bombarded with 17.1 MeV α beams of the Jyväskylä 90-cm cyclotron (γ-spectrum measurements) and the Debrecen 103-cm cyclotron (e$^-$-spectrum measurements).

The energies of γ rays were measured with a 126 cm^3 Ge(HP) detector at 90° to the direction of the bombarding beam. For the γ-ray intensity measurements we have used a 93 cm^3 Ge detector which was placed at 125° to the beam direction. The resolutions [full width at half maximum (FWHM)] of the detectors were $\simeq 3$ keV (at 1332 keV). The spectrometers have been calibrated with ^{133}Ba and ^{152}Eu sources.

For the conversion electron spectrum measurements we have used a superconducting magnetic lens spectrometer with Si(Li) detectors.[23] The energy resolution of the Si(Li) detectors was $\simeq 2.7$ keV (at 976 keV). The background from backscattered electrons was effectively reduced with a swept energy window in the pulse spectrum of the Si(Li) detector. Further background reduction was achieved with antipositron baffles. In order to decrease the background from the β^- decay of ^{112}In, some e$^-$ spectra were measured in coincidence with the rf accelerating voltage signals. The transmission of the spectrometer was about 5% of 4π for the upper detector and about the same for the lower one. For the calibration of the spectrometer an ^{152}Eu source was used.

The conversion electrons were collected by the superconducting magnetic lens spectrometer from a wide range of angles (approximately from $\simeq 40°$ to $\simeq 140°$ to the direction of the bombarding beam). Using the available γ-ray angular distribution coefficients,[5] the solid angle correction factors,[23] and the normalized directional particle parameters, we estimated the effect of angular distribution of electrons on the measured internal conversion coefficients (ICC). The result showed that this effect was usually much less than the statistical uncertainties of ICC's given in Table III. In some exceptional cases, when the effect was strong, greater uncertainties are given.

All measurements were performed with a versatile multichannel analyzer and data display system in Jyväskylä and CAMAC modular units connected to a TPA 11/440 computer in Debrecen. The processing of spectra was done with the TPA 11/440 computer and a modified version of the γ-spectrum-analysis (Ref. 24) program.

III. EXPERIMENTAL RESULTS

Typical γ-ray and internal conversion electron spectra of the (p,n) and (α,n) reactions are shown in Figs. 1 and 2, respectively. The γ-spectrum measurement of the ^{112}Cd + p, ^{113}Cd + p, and ^{114}Cd + p reactions (at $E_p = 4.8$ MeV), the ^{109}Ag$+\alpha$ and ^{107}Ag$+\alpha$ reactions (at $E_\alpha = 17.1$ MeV), and the measurement of the radioactive decay of the products enabled unambiguous γ-ray identification in most cases. The energies and relative intensities of the γ rays assigned to the ^{112}Cd(p,nγ)^{112}In and ^{109}Ag(α,nγ)^{112}In reactions are summarized in Table II.

In the (p,n) studies the γ-ray and conversion-electron intensities were normalized by using the theoretical α_K internal conversion coefficient[25] of the 617.49 keV $2_1^+ \to 0_1^+$ $E2$ transition of ^{112}Cd. With this normalization the known ICC's of the 156.57 keV $M3$ transition[11,18] of ^{112}In, and the 255.06 keV $M1+E2$ and 1024.2 keV $E2$ transitions[26] of ^{113}In have been reproduced.

In the (α,n) studies we have used for normalization the 311.4 keV $M1+E2$ transition of ^{109}Ag(α,α'), for which the ICC is known ($\alpha_K = 0.01751$).[27] With this normali-

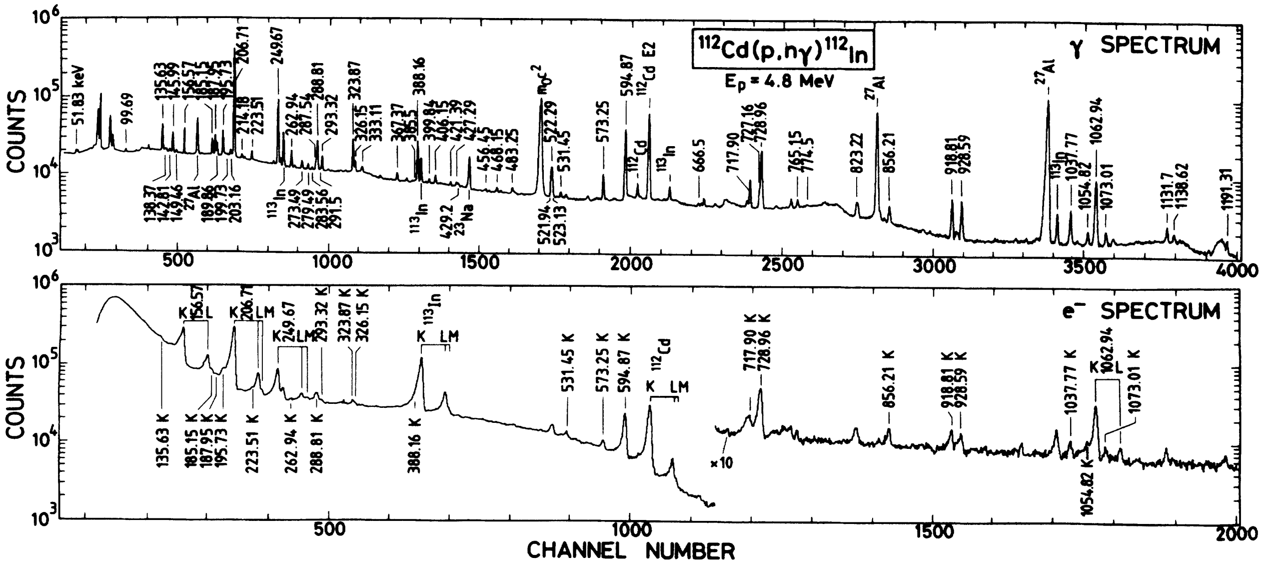

FIG. 1. Typical γ-ray and internal conversion electron spectra of the ^{112}Cd(p,nγ)^{112}In reaction. The energies of γ rays are given only at ^{112}In lines.

zation many formerly determined ICC's of ^{109}Ag and ^{111}In transitions have been reproduced within experimental errors. The ICC's of the ^{112}In transitions are shown in Fig. 3. The exact values of the ICC's and multipolarities are given in Table III.

IV. LEVEL SCHEME OF ^{112}In

A. (p,nγ) reaction

The level scheme construction was based on the energy and intensity balance of transitions and on the former $\gamma\gamma$

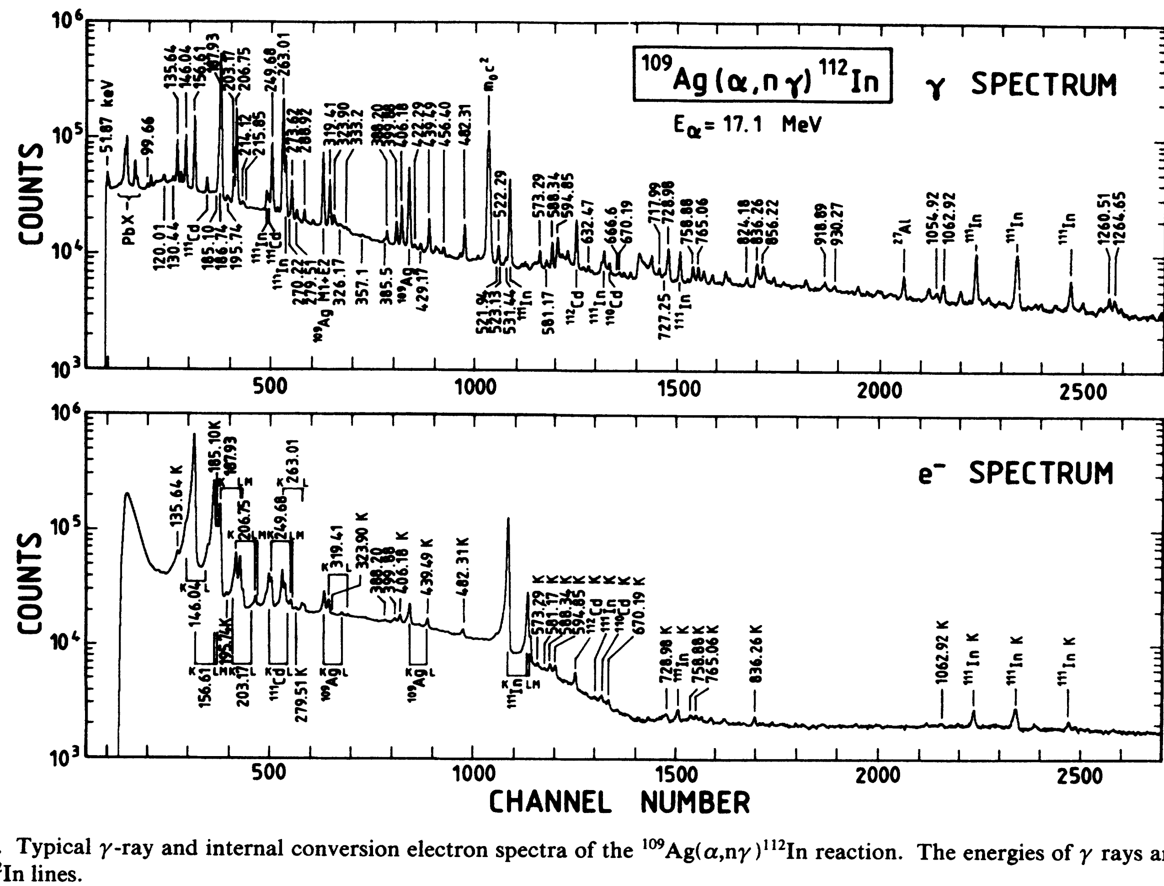

FIG. 2. Typical γ-ray and internal conversion electron spectra of the ^{109}Ag(α,nγ)^{112}In reaction. The energies of γ rays are given only at ^{112}In lines.

TABLE II. The energy (E_γ) and relative intensity (I_γ) of γ rays observed in the ^{112}Cd(p,nγ)^{112}In and ^{109}Ag(α,nγ)^{112}In reactions at $E_p = 4.8$ MeV and $E_\alpha = 17.1$ MeV, respectively.

	^{112}Cd(p,nγ)^{112}In			^{109}Ag(α,nγ)^{112}In	
E_γ [a,b] (keV)	I_γ [b] (relative)	Placement into scheme[c]	E_γ [d] (keV)	I_γ [b] (relative)	Placement into scheme[c]
51.83	0.94(12)	S	51.87(3)	8.2(4)	S'
99.69	0.35(6)		99.66(6)	1.3(1)	
			120.01(4)	1.7(3)	S'
			130.44(4)	1.5(1)	
135.63	4.3(1)	S	135.64(3)	24.4(6)	S'
138.37	0.36(3)	S			
142.81	0.34(3)				
145.99	2.95(10)	S	146.04(3)	30.5(8)	S'
149.46	0.37(3)	S			
156.57	4.2(2)	S	156.61(3)	60(2)	S'
185.15	2.4(1)	S	185.10(3)	17.4(5)	S'
			186.74(4)	95(3)	S'
187.95	3.3(2)	S	187.93(3)	222(6)	S'
189.86	1.8(1)	S			
195.73	4.0(2)	S	195.74(10)	1.9(1)	S'
199.73	0.14(4)	S			
203.16	0.89(5)	S	203.17(3)	11.5(3)	S'
206.71	100(4)	S	206.75(3)	100(3)	S'
214.18	0.56(4)	S	214.12(9)	1.4(1)	S'
			215.85(9)	0.9(1)	
223.51	1.40(8)	S			
249.67	25.2(4)	S	249.68(3)	56(2)	S'
262.94	2.8(1)	S	263.01(3)	172(10)	S'
			270.22(7)	1.3(3)	S'
273.49[e] }	1.16(6)	S	273.49[e] }		S'
273.62[e] }		S	273.62(3)[e] }	18.8(3)	S'
279.49	0.78(4)	S	279.51(3)	2.3(3)	S'
283.56	0.37(4)	S			
287.54	1.56(6)	S			
288.81	6.3(2)	S	288.92(3)	4.7(4)	S'
291.5(2)	0.2(1)	S			
293.32	2.4(1)	S			
			319.41(3)	27.1(13)	S'
323.87	8.2(4)	S	323.90(5)	4.1(2)	S'
326.15	2.0(1)	S	326.19(10)	1.0(2)	S'
333.11	0.92(6)	S	333.2(1)	0.8(2)	S'
			357.1(3)	0.5(2)	
367.37	1.12(6)	S			
385.5(2)	0.16(5)	S	385.5(1)	1.5(1)	S'
388.16	11.4(4)	S	388.20(3)	5.0(3)	S'
399.84	0.60(5)	S	399.88(3)	10.6(4)	S'
406.15	1.29(6)	S	406.18(3)	21.2(7)	S'
421.39	0.52(5)	S			
			422.29(8)	1.4(1)	
427.29	0.65(6)	S			
429.2(1)	0.5(1)	S	429.17(5)	2.3(1)	S'
			439.49(3)	16.5(4)	S'
456.45	0.39(7)	S	456.40(5)	1.7(3)	S'
468.15	0.85(6)	S			
			482.31(3)	17.3(11)	S'
483.25	1.04(7)	S			
521.94[f] }		S	521.94[f] }		S'
522.29[f] }	11.3(9)	S	522.29[f] }	7.4(5)	S'
523.13[f] }		S	523.13[f] }		S'
531.45	1.2(2)	S	531.44(11)	1.9(2)	S'
573.25	6.1(3)	S	573.29(3)	7.2(4)	S'
			581.17(7)	2.7(2)	

TABLE II. (*Continued*).

^{112}Cd(p,nγ)^{112}In			^{109}Ag(α,nγ)^{112}In		
E_γ [a,b] (keV)	I_γ [b] (relative)	Placement into scheme[c]	E_γ [d] (keV)	I_γ [b] (relative)	Placement into scheme[c]
			588.34(3)	11.8(5)	S'
594.87	37.4(17)	S	594.85(3)	11.6(6)	S'
			632.47(7)	2.6(2)	
666.5(1)	0.47(7)	S	666.6(1)	0.8(2)	S'
			670.19(13)	1.7(2)	S'
717.90	7.8(3)	S	717.99(5)	3.5(2)	S'
727.16	4.0(2)	S	727.25(10)	4.4(4)	S'
728.96	28.1(10)	S	728.98(3)	16.7(6)	S'
			758.88(3)	7.8(3)	
765.15	1.6(1)	S	765.06(4)	7.8(3)	S'
774.5(1)	0.34(6)				
823.22(9)	1.4(2)	S			
			824.18(5)	3.6(2)	
			836.26(4)	8.7(5)	
856.21	3.6(2)	S	856.22(6)	3.8(3)	S'
918.81	7.7(2)	S	918.89(8)	3.0(2)	S'
928.59	7.1(2)	S			
			930.27(11)	2.7(2)	
1037.77	5.9(2)	S			
1054.82	1.7(1)	S	1054.92(10)	4.0(3)	S'
1062.94	20.4(8)	S	1062.92(7)	11.2(8)	S'
1073.01	1.6(1)	S			
1131.7(1)	2.3(3)				
1138.62(8)	1.1(2)				
1191.31	1.1(2)				
1260.53[f]		S	1260.51(11)	2.3(4)	S'
			1264.65(9)	7.4(4)	
1279.59[f]		S			

[a]The errors of energies are less than ±0.08 keV, if otherwise not indicated.
[b]Measured at 125° to the beam direction.
[c]S and S': placed into the level scheme of (p,nγ) (Fig. 4) and (α,nγ) reactions, respectively.
[d]Measured at 90° to the beam direction.
[e]The line is doublet according to Samuelson *et al.* (Ref. 5).
[f]The energy was taken from Kohno *et al.* (Ref. 9).

coincidence[4,9] and other[10] results. As the bombarding proton energy was 4.8 MeV, the ^{112}In levels could be excited only up to 1.38 MeV. With the exception of some weak lines, all observed ^{112}In γ rays have been placed into the level scheme.

The proposed level scheme is shown in Fig. 4. The level system agrees well with that of Kohno *et al.*[9] In the ^{112}Cd(p,nγ)^{112}In reaction (at $E_p=4.8$ MeV), high-spin (≥ 5) states cannot be directly excited, nevertheless some of them were seen in our experiments as a result of γ decay of higher-lying low-spin states.

The γ-ray branching ratios are shown in Fig. 4 after the transition energies and multipolarities. These branching ratios are the weighted averages of our (p,nγ) and (α,nγ) results. Some of them are new, the others show rather good agreement with the corresponding data of Kohno *et al.*[9] and Emigh *et al.*[6]

The level spin and parity assignments are based mainly on the measured internal conversion coefficients of transitions and (to a lesser extent) on the Hauser-Feshbach analysis and other arguments. A detailed discussion of the levels can be found in Table IV.

B. (α,nγ) reaction

The ^{112}In level schemes obtained from (p,nγ) and (α,nγ) reactions are similar below 1290 keV excitation energy, but, in the (α,nγ) reaction, some additional high-spin states have appeared owing to the higher angular momentum transfer. The levels are as follows: 670.24 keV $J^\pi=8^+$, 7^+, $(6)^+$; 790.28 keV $(7,8)^+$; 800.56 keV (9^-); 833.10 keV $(6)^+$; 1388.90 keV (10^-). The spin and parity assignments are discussed in Table IV. Most of these additional levels can be identified as members of different p-n multiplets (see Fig. 7).

The 928.62 keV $J^\pi=(0)^-$, 1037.77 keV $(0)^-$, 1150.34 keV (≥ 3), 1212.13 keV $\leq 4^-$, 1212.23 keV (≤ 3), 1279.69 keV $(1-3)^+$, and 1286.28 keV $\leq 3^-$ states were not seen in the (α,nγ) reaction.

V. HAUSER-FESHBACH ANALYSIS

As a result of detailed γ-spectroscopic measurements, the low-energy level scheme of ^{112}In can be considered nearly complete. Thus the cross sections for the neutron groups feeding the ^{112}In levels can be deduced from the γ-ray intensities after corrections for internal conversion. The obtained $\sigma_{\rm LEV}$(p,n) relative cross sections are shown in Fig. 5.

In order to determine the level spins, $\sigma_{\rm LEV}$(p,n) values

TABLE III. Experimental internal conversion coefficient (ICC) and multipolarity of ^{112}In transitions.

		Experimental ICC, α (10^{-2})		Multipolarity	
E_γ (keV)	Shell	^{112}Cd(p,n)^{112}In	^{109}Ag(α,n)^{112}In	Present work	Former ICC results
135.63	K	20(4)	18(2)	M1	
146.04	K		17(4)	M1	
	L		2.2(9)		
156.57	K	540(50)		M3	M3 (Refs. 11 and 18)
	L	136(12)			
185.15	K	7(1)	10(2)	M1	
187.95	K	11(1)	11(1)	E2	E2 (Refs. 3 and 13–15)
	L		2.1(3)		
	M		0.56(6)		
195.73	K	7.3(6)	6.0(6)	M1	
203.17	K		7.2(12)	M1	
	L		0.97(10)		
206.71	K	7.2(6)	5.9(7)	M1	
	L	0.75(6)	0.68(7)		
	M	0.13(1)	0.15(4)		
223.51	K	1.9(5)		E1	
249.67	K	4.1(3)	3.6(4)	M1	
	L	0.54(10)			
	M	0.13(3)			
262.94	K	1.4(3)	1.5(2)	E1+M2	M2 (Ref. 3)
	L		0.15(2)		
279.51	K		2.9(5)	M1	
288.81	K	2.4(5)		M1	
293.32	K	3.0(5)		E2,M1	
319.41	K		2.2(3)	M1	
	L		0.19(3)		
323.87	K	0.6(2)	0.7(2)	E1	
326.15	K	$\leq$1.2		E1	
388.16	K	1.27(12)	1.11(11)	M1,E2	
399.88	K		1.25(15)	M1,E2	
406.18	K		1.23(14)	M1,E2	
439.49	K		0.90(16)	M1,E2	
482.31	K		0.81(13)	M1,E2	
531.45	K	0.6(2)		M1,E2	
573.25	K	0.39(5)	0.42(10)	E2,M1	
581.17	K		0.47(12)	M1,E2	
588.34	K		0.46(11)	M1,E2	
594.87	K	0.45(4)	0.46(6)	M1,(E2)	
670.19	K		0.36(8)	M1	
717.90	K	0.09(1)		E1	
728.96	K	0.099(15)	0.100(9)	E1	
758.88	K		0.24(5)	M1	
765.06	K		0.25(4)	M1	
836.26	K		0.20(5)	M1,(E2)	
856.21	K	0.150(35)		E2,(M1)	
918.81	K	0.063(7)		E1	
928.59	K	0.057(6)		E1	
1037.77	K	0.044(6)		E1	
1054.82	K	0.10(2)		M1,E2	
1062.94	K	0.088(12)	0.083(13)	E2	
	L	0.010(1)			
1073.01	K	0.11(2)		M1,E2	

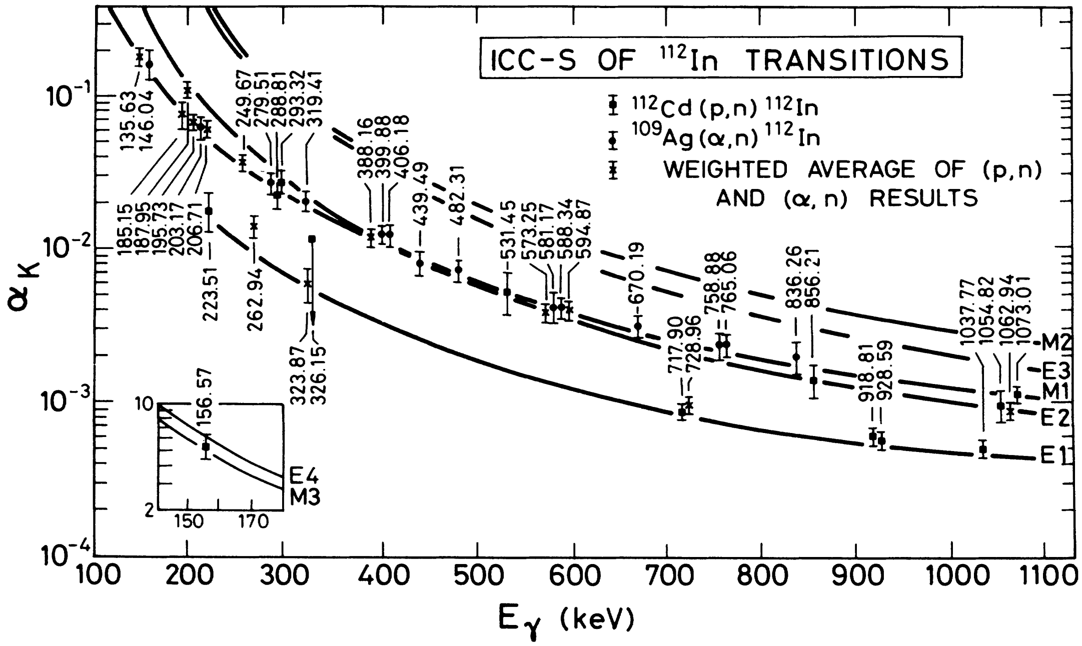

FIG. 3. The experimental α_K internal conversion coefficients of ^{112}In transitions (data symbols with error bars) as a function of γ-ray energy (E_γ). The curves show theoretical results (Ref. 25).

were calculated at the 4.8 MeV bombarding proton energy using the CINDY (Ref. 29) program, which was based on the compound nuclear reaction model. The transmission coefficients were calculated using the optical-model parameter set of Wilmore and Hodgson[30] for neutrons and of Perey[31] (modified by Gyarmati *et al.*[32]) for protons. The parameters of the optical potentials are given in Table V. Besides the neutron channels, (p,γ) and some (p,p′) channels were included. The Moldauer width fluctuation correction was taken into account.

The experimental cross sections were normalized so that the cross sections of the 206.72 keV 2^+ and 456.45 keV 3^+ states should reproduce the corresponding theoretical values. All experimental cross sections were multiplied by the same factor. The experimental and theoretical results are compared in Fig. 5.

We remark that the theoretical σ(p,n) values are interdependent, since changing the spin (and parity) of any individual level requires the redistribution of the outgoing flux through the remaining levels. Nevertheless, the variation of the spin and parity of a level can cause only a few percent change in the cross section of others (see the approximate bandwidths of theoretical data in Fig. 5).

VI. PROTON-NEUTRON MULTIPLET STATES IN ^{112}In

In the $^{112}_{49}\mathrm{In}_{63}$ nucleus we may expect excitations of the odd proton and odd neutron and the coupling of different single particle states. In zeroth order approximation the energies of ^{112}In multiplets can be obtained by the addition of energies of the odd proton and odd neutron states.

The energies of proton hole states may be taken from the neighboring $^{111}_{49}\mathrm{In}_{62}$ and $^{113}_{49}\mathrm{In}_{64}$ nuclei. According to the (d,^{3}He) reaction studies of Conjeaud *et al.*,[33] the (α,t) and (^{3}He,d) proton transfer experiments of Markham and Fulbright,[34] the g factor and nuclear moment measurements of Hagn and Zech[35] and Ulm *et al.*[36] (for the ground states), as well as the intermediate coupling unified model calculations of Atalay and Chiao-Yap,[37] and weak-coupling calculations of Smits and Siemssen (for ^{115}In),[38] the main components of the $\frac{9}{2}^+$ ground, $\frac{1}{2}^-$ first, and $\frac{3}{2}^-$ second excited states of the ^{111}In and ^{113}In nuclei have $\pi\tilde{g}_{9/2}$, $\pi\tilde{p}_{1/2}$, and $\pi\tilde{p}_{3/2}$ configurations, respectively. Nevertheless, especially the $\frac{3}{2}{}_1^-$ state is not pure (Conjeaud *et al.*[33]).

The energies of the neutron states were taken from the neighboring $^{113}_{50}\mathrm{Sn}_{63}$ nucleus. On the basis of (p,d) (Cavanagh *et al.*[39] and Fleming[40]) and (d,p) (Borello *et al.*[41]) neutron transfer experiments and pairing plus quadrupole force model calculations of Sorensen,[42] we have adopted for the main components of the lowest states of ^{113}Sn the following configurations: ground state $J^\pi=\frac{1}{2}^+$, $\nu\tilde{s}_{1/2}$; 77.3 keV $\frac{7}{2}^+$, $\nu\tilde{g}_{7/2}$; 409.8 keV $\frac{5}{2}^+$, $\nu\tilde{d}_{5/2}$; 498.0 keV $\frac{3}{2}^+$, $\nu\tilde{d}_{3/2}$; and 739.4 keV $\frac{11}{2}^-$, $\nu\tilde{h}_{11/2}$.

The configurations of the main components of the low-lying ^{111,113}In and ^{113}Sn states are shown in Fig. 6(a). Here we describe the low-lying levels of ^{112}In by using the parabolic rule derived from the cluster-vibration model. In this approximation the proton-neutron residual interaction is a consequence of the quadrupole and spin vibration phonon exchange between the proton and neutron through the nuclear core. As a result of this interaction the $E[(j_p,j_n)J]$ energies of the multiplets split as a function of the nuclear spin (J) (Paar[43]):

$$E[(j_p,j_n)J]=E_{j_p}+E_{j_n}+\delta E_2+\delta E_1\ , \tag{1}$$

$$\delta E_2=-\alpha_2\mathcal{V}\frac{[J(J+1)-j_p(j_p+1)-j_n(j_n+1)]^2+J(J+1)-j_p(j_p+1)-j_n(j_n+1)}{2j_p(2j_p+2)2j_n(2j_n+2)}+\mathcal{V}\frac{\alpha_2}{12}\ , \tag{2}$$

$$\delta E_1=-\alpha_1\xi\frac{J(J+1)-j_p(j_p+1)-j_n(j_n+1)}{(2j_p+2)(2j_n+2)}\ . \tag{3}$$

Here E_{j_p} and E_{j_n} denote the quasiproton and quasineutron energies, respectively, which were taken from the experimental data of the neighboring nuclei [see Fig. 6(a)]. $(j_p,j_n)J=(j_p-j_n),\ldots,(j_p+j_n)$, where j is the total angular momentum quantum number of the nucleon and α_2 and α_1 are the quadrupole and spin-vibrational coupling strengths, respectively. The definition of $\mathcal{V}$ and ξ coefficients are given in Ref. 43.

The dependence of the coupling strengths on the occupation probability of levels may be described by the following approximation formulae

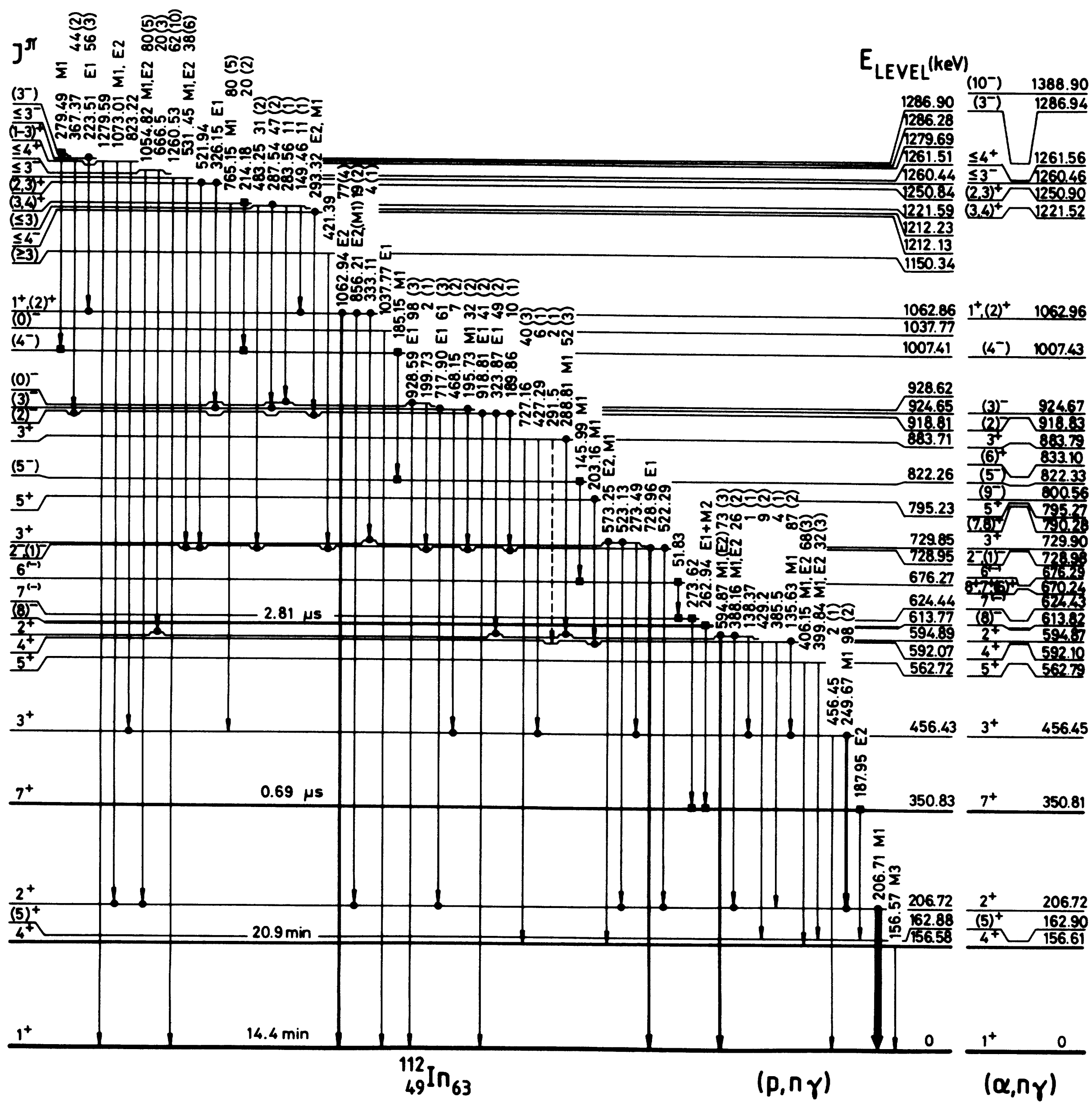

FIG. 4. The proposed level scheme of ^{112}In from ^{112}Cd(p,nγ)^{112}In and ^{109}Ag(α,nγ)^{112}In reactions. Solid circles at the ends of arrows show $\gamma\gamma$-coincidence relations according to Kohno *et al.* (Ref. 9). Some additional $\gamma\gamma$ coincidences are shown with solid squares on the basis of (α,nγ) study of Eibert (Ref. 4).

TABLE IV. Spin and parity (J^{π}) assignment to ^{112}In levels.

Level energy (keV)	J^{π}	Basis of the J^{π} assignment, comments
0	1^+	Atomic beam experiments (Ref. 28) and $\log ft = 4.1$ for β^- decay to 0^+ level of ^{112}Sn (Ref. 10).
156.61(3)	4^+	Atomic beam experiments (Ref. 28), 156.57 keV γ is $M3$ (Refs. 11 and 18 and present work), isomeric state with $T_{1/2} = 20.9$ min (Ref. 10).
162.90(4)	$(5)^+$	$E2$ γ transition (present work and Refs. 13–15 and 3) from 7^+, 350.81 keV level, expected 5^+ member of the $\pi\tilde{g}_{9/2}\nu\tilde{s}_{1/2}$ doublet, large C^2S from (^{3}He,d) and (p,d) suggests doublet structure of the 157 level (not resolved 4^+ and 5^+ states) (Refs. 6, 7, and 10).
206.72(2)	2^+	$M1$ γ to 1^+ ground state; excitation function, γ-ray angular distribution, and γ linear polarization measurements of Adachi *et al.* (Ref. 8); $l_n = 2+4$ from (p,d) (Refs. 6 and 7), expected 2^+ member of the $\pi\tilde{g}_{9/2}\nu\tilde{g}_{7/2}$ multiplet.
350.81(5)	7^+	$l_n = 2$ from (p,d) (Refs. 6 and 7), only $J = 7$ agrees with shell model analysis of the experimental g factor (Refs. 13–15 and 10), expected 7^+ member of the $\pi\tilde{g}_{9/2}\nu\tilde{d}_{5/2}$ multiplet, Hauser-Feshbach analysis suggests high spin.
456.45(2)	3^+	Strong $M1$ transition to 2^+ state; weak transition to the 1^+ ground state; γ-ray angular distribution and linear polarization measurement of Adachi *et al.* (Ref. 8), $l_n = 2+4$ in (p,d) (Refs. 6 and 7); expected 3^+ member of the $\pi\tilde{g}_{9/2}\nu\tilde{g}_{7/2}$ multiplet.
562.79(4)	5^+	$l_n = 2$ from (p,d) (Refs. 6 and 7); $M1,E2$ transitions to 4^+ $(5)^+$ states; the transition to 156.58 keV 4^+ state is dipole (Ref. 6); Hauser-Feshbach analysis: $J = 5$, expected 5^+ member of the $\pi\tilde{g}_{9/2}\nu\tilde{d}_{3/2}$ multiplet.
592.10(4)	4^+	Strong $M1$ transition to 3^+ state, weak transitions to 2^+ and $(5)^+$ states; $l_n = 2+4$ from (p,d) (Refs. 6 and 7), no γ to 1^+ level; Hauser-Feshbach analysis: $J = 4$; Kohno *et al.* (Ref. 9) obtained $J = 4$ from excitation function and γ-ray angular distribution measurements; expected 4^+ member of the $\pi\tilde{g}_{9/2}\nu\tilde{g}_{7/2}$ multiplet.
594.87(2)	2^+	$M1,E2$ transition to 2^+; $M1(E2)$ transition to 1^+ levels; Hauser-Feshbach analysis: $J = 2$ (or 1); γ to 3^+ state; $l_n = 2+4$ from (p,d) (Refs. 6 and 7); from excitation function, γ-ray angular distribution and linear polarization measurement Kohno *et al.* (Ref. 9) determined $J^{\pi} = 2^+$ value; expected 2^+ member of the $\pi\tilde{g}_{9/2}\nu\tilde{d}_{5/2}$ multiplet.
613.82(6)	$(8)^-$	$E1+M2$ γ to 7^+, Peker (Ref. 10) adopted $J = (8)^-$ from Q and g-factor measurements (and calculations), systematics of levels; the $M2$ character of the 262.9 keV transition (Ref. 3); expected 8^- member of the $\pi\tilde{g}_{9/2}\nu\tilde{h}_{11/2}$ multiplet.
624.43(6)	$(7)^-$	273.62 keV γ is $\Delta J = 0$ dipole transition (Ref. 10); systematics of odd-odd In levels; possible $l_n = 5$ from (p,d) (Refs. 6 and 7).
670.24(6)	$8^+,7^+,(6)^+$	319.41 keV $M1\gamma$ to 350.81 keV 7^+ level [in coincidence (Ref. 4)]; $l_n = 4$ from (p,d) reaction (Refs. 6 and 7); expected 8^+ member of the $\pi\tilde{g}_{9/2}\nu\tilde{g}_{7/2}$ multiplet.
676.29(6)	$6^{(-)}$	51.83 keV γ is $\Delta J = 1$ transition (Ref. 10); systematics of odd-odd In levels; possible $l_n = 5$ from (p,d) (Refs. 6 and 7).
728.98(3)	$2^-,(1)^-$	$E1$ transition to 1^+ ground state; Hauser-Feshbach analysis: $J = 2$ (or 1); γ to 2^+; Kohno *et al.* (Ref. 9) obtained $J^{\pi} = 1^+$ or 2.
729.90(3)	3^+	$E2,M1$ γ to 4^+; γ-*s* to 2^+ and 3^+; Hauser-Feshbach analysis: $J = 3$; possible $l_p = 2$ from (^{3}He,d) (Refs. 6 and 7); Kohno *et al.* (Ref. 9) obtained $J^{\pi} = 3^{(+)}$.
790.28(6)	$(7,8)^+$	439.49 keV 91(2) $M1,E2$ γ to 350.81 keV 7^+ level; 120.01 keV 9(2) γ to 670.22 keV $8^+,7^+,(6)^+$ state; $l_n = 4+2$ from (p,d) reaction (Refs. 6 and 7) expected 7^+ member of the $\pi\tilde{g}_{9/2}\nu\tilde{g}_{7/2}$ multiplet.
795.27(5)	5^+	$l_n = 2+4$ from (p,d) (Refs. 6 and 7); $M1$ γ to 4^+ state; Hauser-Feshbach analysis: $J \geq 4$; Kohno *et al.* (Ref. 9) give $J^{\pi} = 5^{(-)}$, expected 5^+ member of the $\pi\tilde{g}_{9/2}\nu\tilde{g}_{7/2}$ multiplet.
800.56(7)	(9^-)	Strong 186.74 keV γ to $(8)^-$ state; the 186.9 γ is $\Delta J = 1$ transition (Ref. 10); systematics of odd-odd In isotopes.
822.33(7)	(5^-)	$M1$ transition to $6^{(-)}$ state; systematics of levels of odd-odd In isotopes.
833.10(5)	$(6)^+$	670.19 keV 9(1) $M1$ γ to $J^{\pi} = (5)^+$; 482.31 keV 85(5) $M1,E2$ γ to $J^{\pi} = 7^+$; 270.22 keV 6(2) γ to $J^{\pi} = 5^+$ states. Emigh *et al.* (Ref. 6) and Peker (Ref. 10) give $J^{\pi} = (6,8)$ values. $l_n = 2+4$ in (p,d) reaction (Refs. 6 and 7). Probable 6^+ member of the $\pi\tilde{g}_{9/2}\nu\tilde{g}_{7/2}$ multiplet.
883.79(4)	3^+	Strong $M1$ γ to 2^+ state; γ-*s* to 3^+ and 4^+ states; Hauser-Feshbach analysis: $J = 3$ (or 4); Kohno *et al.* (Ref. 9): $J^{\pi} = 3^+$; $l_n = 2$ from (p,d) (Refs. 6 and 7); expected 3^+ member of the $\pi\tilde{g}_{9/2}\nu\tilde{d}_{5/2}$ multiplet.
918.83(3)	$(2)^-$	$E1$ γ-*s* to 1^+ and 2^+ levels; Hauser-Feshbach analysis: $J^{\pi} = (2)^-$; $l_p = 1$ from (^{3}He,d) (Refs. 6 and 7); Kohno *et al.* (Ref. 9) give $J^{\pi} = 1^-,2^+$.
924.67(4)	$(3)^-$	$E1$ γ to 2^+; $M1$ γ to $2^-,(1)^-$ states; Hauser-Feshbach analysis: $J = 3$ or 0; γ to 3^+ state.
928.62(4)	$(0)^-$	$E1$ γ to 1^+; γ to $2^-,(1)^-$ states; Hauser-Feshbach analysis: $J = 0$ or 3.
1007.43(7)	(4^-)	$M1$ γ to (5^-), observed in (α,d) (Ref. 5); systematics of odd-odd In level schemes;

TABLE IV. (*Continued*).

Level energy (keV)	J^{π}	Basis of the J^{π} assignment, comments
		Hauser-Feshbach analysis: $J=4$ or 5.
1037.77(7)	$(0)^-$	$E1$ γ to 1^+, Hauser-Feshbach analysis: $J=0$ (or 3).
1062.96(5)	$1^+,(2)^+$	$E2$ transition to 1^+; $E2,(M1)$ transition to 2^+ states; γ to 3^+ state; Hauser-Feshbach analysis suggests $J^{\pi}=1^+$; Kohno *et al.* (Ref. 9) determined $J^{\pi}=2^+,1^-$.
1150.34(10)	(≥ 3)	γ to $2^-,(1)^-$ level; Hauser-Feshbach analysis: $J\geq 3$.
1212.13(5)	$\leq 4^-$	$E2,M1$ transition to $(2)^-$ state.
1212.23(4)	(≤ 3)	γ-*s* to $2^-,(1)^-$, $(3)^-$, $(0)^-$, and $1^+,(2)^+$ states.
1221.52(5)	$(3,4)^+$	$M1$ γ to 3^+; γ to (4^-) states.
1250.90(6)	$(2,3)^+$	$E1$ transition to $(3)^-$ state; γ to $2^-,(1)^-$ state; $l_n=0+2$ from (p,d) (Refs. 6 and 7).
1260.46(9)	$\leq 3^-$	$M1,E2$ γ to $2^-,(1)^-$ state; γ to 1^+ ground state.
1261.56(8)	$\leq 4^+$	$M1,E2$ transition to 2^+; γ to 2^+ states.
1279.69(6)	$(1-3)^+$	$M1,E2$ transition to 2^+ state; γ-*s* to 3^+ and 1^+ (ground) states.
1286.28(4)	$\leq 3^-$	$E1$ γ to $1^+,(2)^+$ state; γ to $(2)^-$.
1286.94(8)	(3^-)	$M1$ transition to (4^-) state, systematics of levels of odd-odd In nuclei.
1388.90(8)	(10^-)	588.34 keV $M1,E2$ transition to (9^-) state, systematics of odd-odd In nuclei.

$$\alpha_2(j_p,j_n)=\alpha_2^{(0)}\,|\,(U_{j_p}^2-V_{j_p}^2)(U_{j_n}^2-V_{j_n}^2)\,| \;, \tag{4}$$

$$\alpha_1(j_p,j_n)=\alpha_1^{(0)} \;, \tag{5}$$

where V_j^2 is the probability of occupation of the j level, $U_j^2=1-V_j^2$. The knowledge of occupation probability is important also for the description of the $\mathcal{V}$ parameter. The occupation probabilities of the quasiparticle states were obtained from the systematics of the experimental V^2 values ([1,34,40,44–47,19] and others). The values used in the calculations are as follows:

$V^2(\pi g_{9/2})=0.87$, $V^2(\nu g_{7/2})=0.78$, $V^2(\nu d_{5/2})=0.70$,

$V^2(\nu d_{3/2})=0.17$, $V^2(\nu h_{11/2})=0.18$.

A consistent description of different ^{110}In (Ref. 48), ^{112}In, ^{114}In, and ^{116}In (Ref. 49) multiplets was achieved with $\alpha_2^{(0)}=8.7$ MeV. This is a reasonable value, taking into account that for the close even-even nuclei $\alpha_2^{(0)}(^{112}\mathrm{Sn})=5.1$, $\alpha_2^{(0)}(^{114}\mathrm{Sn})=4.1$, and $\alpha_2^{(0)}(^{112}\mathrm{Cd})=21.4$ values can be obtained on the basis of the formula $\alpha_2^{(0)}=382\ \beta_2^2(\hbar\omega_2)^{-1}$ ("natural parametrization").[50] Here $\hbar\omega_2$ is the energy of the first 2^+ state (in MeV) and β_2 is the deformation parameter.

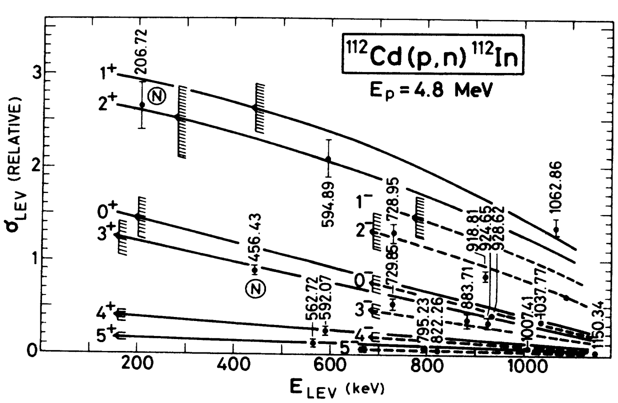

FIG. 5. The experimental relative cross sections (σ_{LEV}) of the ^{112}Cd(p,nγ)^{112}In reaction (dots with error bars) as a function of the ^{112}In level energy (E_{LEV}). The curves (bands) show Hauser-Feshbach theoretical results.

The $\alpha_1^{(0)}$ value was calculated from the expression $\alpha_1^{(0)}\approx 15/A\approx 0.13$ MeV, where A is the atomic mass number. This formula proved to be successful also in the case of ^{110}In, ^{114}In, and ^{116}In.[48,49]

At each multiplet we used one overall normalization term, which pushed up (or down) all members of the given multiplet with the same energy value. The results of the calculations are shown in Figs. 6(b) and 6(c).

The experimental level scheme of ^{112}In is shown in Fig. 6(d), which was compiled on the basis of present results and of the former (d,t),[1] (p,d),[6,7] (^{3}He,d),[6,7] (α,nγ), and (^{6}Li,4nγ) (Ref. 4) reaction studies. The most probable configuration assignments are shown in Fig. 6 with connection lines between the experimental and theoretical levels.

Between the neighboring $J\rightarrow J\pm 1$ members of the same p-n multiplet one can expect strong $M1$ transitions. The experimental results and the expected configurations are shown in Fig. 7. The reasons of configuration assignments are explained according to proton-neutron multiplets.

The $\pi g_{9/2},\nu g_{7/2}$ multiplet. The neutron transfer experiments and the existence of the 203.16, 135.63, 249.67, and 206.71 keV strong $M1$ γ-ray cascade transitions indicate, that the $1^+,2^+,\ldots,5^+$ members of the multiplet can be identified with the ground state 1^+, 206.72 keV 2^+, 456.45 keV 3^+, 592.10 keV 4^+, and 795.27 keV 5^+ states. The experimental data are well described by the calculations.

At opposite j_p and j_n alignment one can expect strong overlap between the $5g_{9/2}$ proton and $5g_{7/2}$ neutron wave functions (spin-orbit partner states). Consequently, the proton-neutron interaction will be strong and the 1^+

TABLE V. Optical-model parameters used in this work. (The V, W, and $V_{s.o.}$ potential depths are given in MeV and the r range and a diffuseness parameters in fm. E is the energy of bombarding proton or outgoing neutron in MeV.)

	V	W	$V_{s.o.}$	r_{RE}	r_{IM}	a_{RE}	a_{IM}	Refs.
p+^{112}Cd	65.8−1.13E	11.5	7.5	1.25	1.5	0.65	0.47	31 and 32
n+^{112}In	47.1−0.267E−0.00118E^2	9.52−0.53E	7.5	1.28	1.24	0.66	0.48	30

state sinks down, this will be the ground state. A similar phenomenon was observed also in the case of ^{114}In and ^{116}In.

The experimental information is insufficient for the sure identification of the 6^+, 7^+, and 8^+ members of the multiplet. Nevertheless there are candidates for these states, the experimental 833.10 keV $(6)^+$, 790.28 keV $(7,8)^+$, and 670.24 keV, $8^+,7^+,(6)^+$ levels, respectively, which have $\pi\tilde{g}_{9/2},\nu\tilde{g}_{7/2}$ components. (See also Sec. VII.)

The $\pi\tilde{g}_{9/2},\nu\tilde{s}_{1/2}$ *doublet.* The proton and neutron transfer experiments[6,7] indicate, that the 156.61 keV 4^+ and 162.90 keV $(5)^+$ states are the 4^+ and 5^+ members of this doublet, respectively.

According to the parabolic rule calculations, the 4^+ member of this doublet has higher energy than the 5^+ one in the ^{116,114,112,110}In nuclei. This prediction is approved by the experiment in the case of ^{116,114}In,[46] but not in ^{112,110}In. The reason of this discrepancy may be the stronger configuration mixing of the $\pi\tilde{g}_{9/2}\nu\tilde{s}_{1/2}$, $\pi\tilde{g}_{9/2}\nu\tilde{d}_{5/2}$, and $\pi\tilde{g}_{9/2}\nu\tilde{d}_{3/2}$ 4^+ and 5^+ states in ^{112,110}In than in ^{116,114}In.

The $\pi\tilde{g}_{9/2},\nu\tilde{d}_{5/2}$ *multiplet.* The 2^+ and 3^+ members of this multiplet can be identified very likely with the 594.87 keV 2^+ and 883.79 keV 3^+ states, respectively. The configuration assignments are supported by the (p,d) reaction study of Emigh *et al.*[6,7] and by the strong $M1$ transition between the levels.

The available experimental data do not allow a reliable identification of the 4^+, 5^+, and 6^+ members of this multiplet. Nevertheless there are candidates for these states, e.g., the positive parity 1003 and 1142 keV levels, which have $\pi\tilde{g}_{9/2},\nu\tilde{d}$ components (the spins are unknown).

The experimental equivalent of the 7^+ multiplet member is very likely the 350.81 keV 7^+ level. The (p,d) experiments[6,7] indicate $\pi\tilde{g}_{9/2},\nu\tilde{d}$ configuration for this state, and the experimental g factor of the level ($g_{exp}=0.675\pm0.006$) can be reproduced if we suppose $(\pi g_{9/2},\nu d_{5/2})7^+$ configuration ($g_{theor}=0.681$) (Ionescu-Bujor *et al.*[13–15] and Peker[10]).

The $\pi\tilde{g}_{9/2},\nu\tilde{d}_{3/2}$ *multiplet.* The minimum energy 5^+ member of this multiplet corresponds very likely to the experimental 562.79 keV 5^+ state, which has $\pi\tilde{g}_{9/2},\nu\tilde{d}$ configuration.[6,7] The experimental equivalent of the 4^+ member is probably the 923 keV positive parity state (ex-

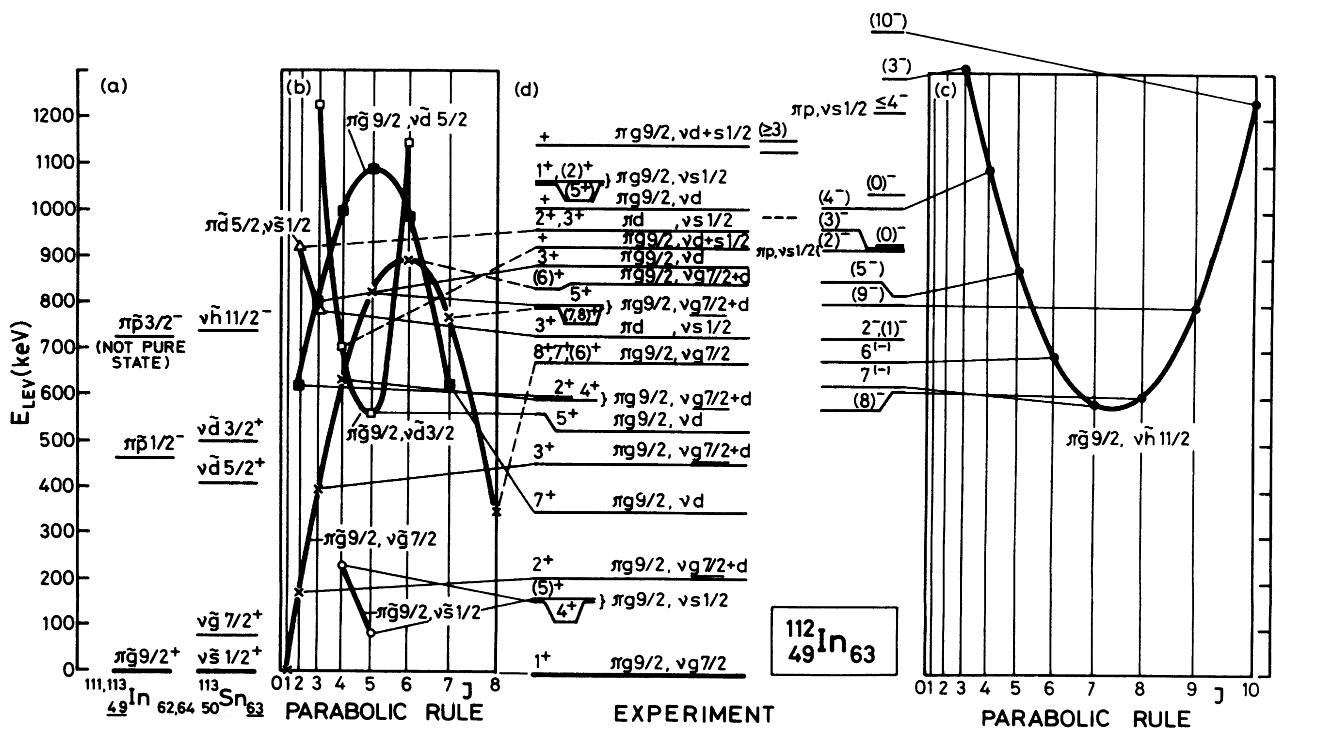

FIG. 6. Proton-neutron quasiparticle multiplet states in ^{112}In. (a) Experimental level energies and configurations of the lowest states of ^{111,113}In and ^{113}Sn nuclei. (b) and (c) Results of the parabolic rule calculation, separately for the positive and negative parity levels. On the abscissa $J(J+1)$ is shown, where J is the spin of the state. (d) Experimental results on ^{112}In levels below 1200 keV.

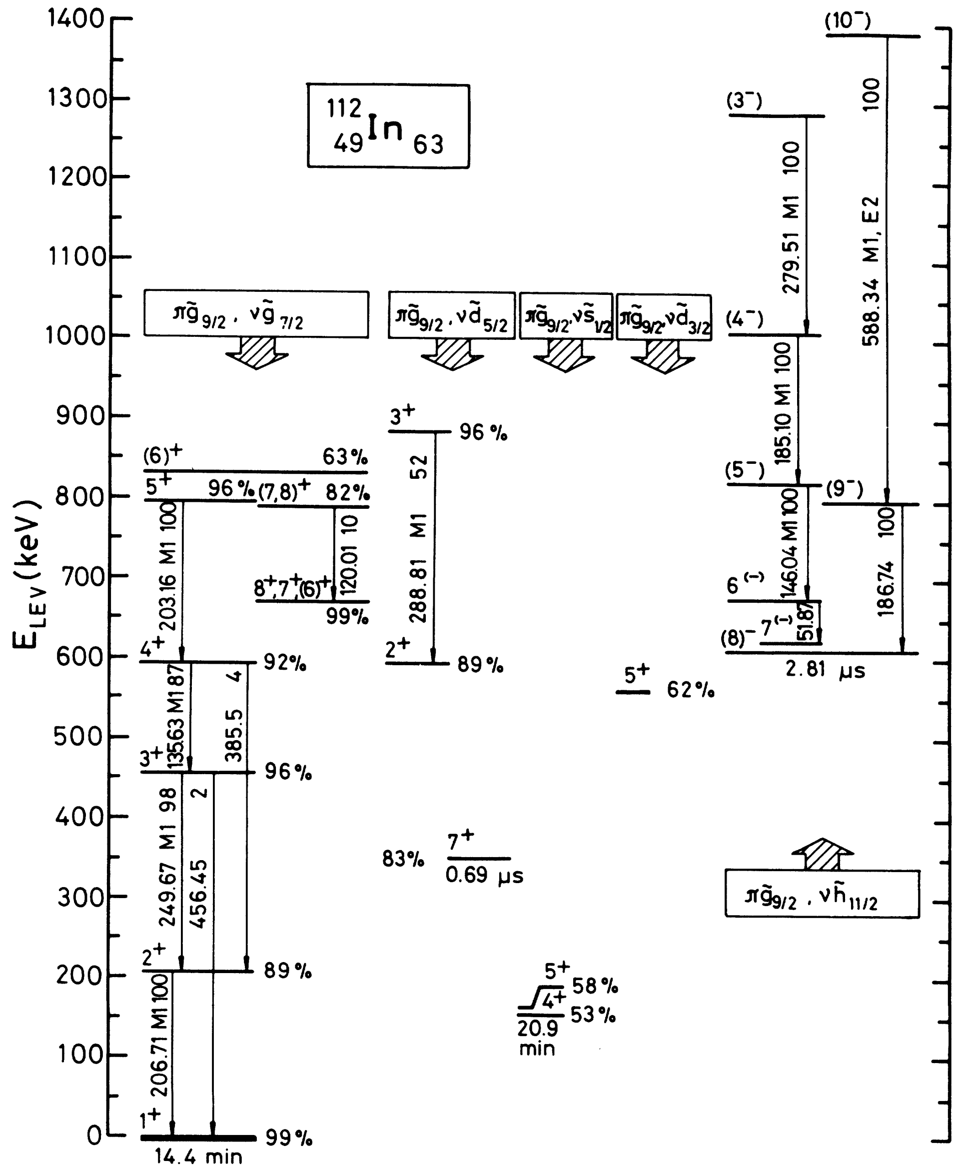

FIG. 7. Proton-neutron multiplet states in ^{112}In and the transitions between the different members of the same multiplet. The percental data at the levels show the total strength of the given configuration in the wave function according to the IBFFM/OTQM calculation. All other data are experimental ones. Behind the transition energies and multipolarities the γ-branching ratios are given.

plained in detail in Sec. VII). Unfortunately the experimental data are insufficient for the identification of the 3^+ and 6^+ multiplet members. According to nucleon transfer experiments the positive parity 1003 and 1142 keV levels have $\pi\tilde{g}_{9/2},\nu\tilde{d}$ components.

The $\pi\tilde{d}_{5/2},\nu\tilde{s}_{1/2}$ intruder doublet. The proton transfer experiments indicate $\pi\tilde{d},\nu\tilde{s}_{1/2}$ configuration for the 955 keV 2^+, 3^+ and 729.90 keV 3^+ states.[6,7] According to the parabolic rule calculations the 2^+ state has higher energy than the 3^+ one, which seems to be in agreement with the experimental data.

The $\pi\tilde{g}_{9/2},\nu\tilde{h}_{11/2}$ multiplet. The $3^-,4^-,\ldots,10^-$ members of this multiplet were identified with the experimental 1286.94 keV (3^-), 1007.43 keV (4^-), 822.33 keV (5^-), 676.29 keV $6^{(-)}$, 624.43 keV $7^{(-)}$, 613.82 keV $(8)^-$, 800.56 keV (9^-), and 1388.90 keV (10^-) levels in the work of Eibert *et al.*[4] on the basis of excitation functions, angular distribution coefficients, systematics, and theoretical expectations. According to our measurements the 146.04, 185.10, and 279.51 keV transitions have *M*1 character (see Fig. 7), which supports the former identification. The parabolic rule calculations well reproduce the energy splitting of the multiplet as a function of $J(J+1)$.

The lowest 0^- state, the experimental 928.62 keV $J^\pi=(0)^-$ level belongs probably to the $\pi\tilde{p}_{1/2}\nu\tilde{s}_{1/2}$ multiplet. This identification is supported also by the (^{3}He,d) reaction studies, which show $\pi\tilde{p}\nu\tilde{s}_{1/2}$ configuration for the 915 keV level.[6] According to the parabolic rule calculation the 0^- member of the $\pi\tilde{p}_{1/2}\nu\tilde{s}_{1/2}$ multiplet has lower energy than the 1^- one.

In order to identify the 1^- member of the $\pi\tilde{p}_{1/2}\nu\tilde{s}_{1/2}$ multiplet and the members of the $\pi\tilde{p}_{1/2}\nu\tilde{g}_{7/2}$, $\pi\tilde{p}_{3/2}\nu\tilde{s}_{1/2}$, etc., multiplets more experimental information is needed.

Altogether $\sim$21 members have been identified in the $\pi\tilde{g}_{9/2}\nu\tilde{g}_{7/2}$, $\pi\tilde{g}_{9/2}\nu\tilde{s}_{1/2}$, $\pi\tilde{g}_{9/2}\nu\tilde{d}_{5/2}$, $\pi\tilde{g}_{9/2}\nu\tilde{d}_{3/2}$, $\pi\tilde{d}_{5/2}\nu\tilde{s}_{1/2}$, and $\pi\tilde{g}_{9/2}\nu\tilde{h}_{11/2}$ multiplets. The energies of these multiplet states were reproduced by the parabolic rule calculations with $\sim$81 keV rms deviation (after the linear normalization shifts), using the same $\alpha_2^{(0)}=8.7$ and $\alpha_1^{(0)}=0.13$ parameters for all multiplets.

The parabolic rule calculations served as a guide for the identification of the low-lying p-n multiplet states. At higher excitation energies many other states are to be expected, e.g., phonon excitation of the core plus quasiparticle states, intruder and multiparticle levels, etc.

VII. CALCULATIONS FOR ^{112}In IN IBFFM/OTQM

A detailed calculation of the energy spectrum and electromagnetic properties of the ^{112}In nucleus was performed in the interacting boson-fermion-fermion model (IBFFM)/odd-odd truncated quadrupole phonon model (OTQM).[20,51]

The IBFFM Hamiltonian reads[20,51]

$$H_{\rm IBFFM}=H_{\rm IBFM}({\rm p})+H_{\rm IBFM}({\rm n})-H_{\rm IBM}+H_{\rm res}({\rm p,n}) \ . \qquad (6)$$

Here $H_{\rm IBM}$ denotes the IBM Hamiltonian;[52] $H_{\rm IBFM}$(p) and $H_{\rm IBFM}$(n) denote the IBFM Hamiltonian[53] for odd-even nuclei with an odd proton and an odd neutron, respectively; $H_{\rm res}$(p,n) is the proton-neutron residual interaction.

In the quadrupole phonon representation the equivalent OTQM Hamiltonian reads[20,51]

$$H_{\rm OTQM}=H_{\rm PTQM}({\rm p})+H_{\rm PTQM}({\rm n})-H_{\rm TQM}+H_{\rm res}({\rm p,n}) \ . \qquad (7)$$

Here $H_{\rm TQM}$ denotes the SU(6) quadrupole phonon model (TQM) Hamiltonian;[54] $H_{\rm PTQM}$(p) and $H_{\rm PTQM}$(n) denote the PTQM Hamiltonian[55] for odd-even nuclei with an odd proton and odd neutron, respectively; $H_{\rm res}$(p,n) is the proton-neutron residual interaction.[56] In the computer code IBFFM/OTQM (Ref. 57) the following residual interactions are incorporated: delta, spin-spin delta, multipole-multipole, spin-spin, and tensor interactions. In the present calculations we have used only the delta and spin-spin interactions: $H_{\rm res}=4\pi\delta({\bf r}_{\rm p}-{\bf r}_{\rm n})[v_D+v_S\boldsymbol{\sigma}_{\rm p}\boldsymbol{\sigma}_{\rm n}]$, where v_D and v_S are the parameters of the Wigner and Bartlett forces, δ is the Dirac δ function, ${\bf r}_{\rm p}$ and ${\bf r}_{\rm n}$ are the position vectors of the proton and neutron, respectively, and the $\boldsymbol{\sigma}$-s are the Pauli spin matrices.

The IBFFM Hamiltonian was diagonalized in the basis

$$|(j_{\rm p},j_{\rm n})j_{\rm pn},n_s n_d v_d I;J\rangle \ , \qquad (8)$$

or the QTQM Hamiltonian in the basis

$$|(j_{\rm p},j_{\rm n})j_{\rm pn},n v I;J\rangle \ . \qquad (9)$$

Here, the quasiproton with angular momentum $j_{\rm p}$ and quasineutron with angular momentum $j_{\rm n}$ are coupled to the angular momentum $j_{\rm pn}$. This angular momentum is coupled with the boson angular momentum I to the total angular momentum J. In the basis (8), the labels n_s, n_d, and v_d denote the number of s bosons, number of d bosons, and additional quantum numbers when needed to distinguish the states with the same values of n_d,I, respectively. In the basis (9), the label n denotes the number of quadrupole phonons and v the additional quantum number when needed to distinguish the states with the same values of n,I. The basis (9) trivially follows from (8) by omitting n_s and using $n_d=n$, $v_d=v$. Thus, the total number of s and d bosons in the basis (8), $N=n_s+n_d$, is equal to the maximum number of quadrupole phonons in the basis (9). Here we perform the computation in the OTQM representation.[57]

In the present calculation for ^{112}In the parametrization was taken as follows. The BCS occupation probabilities are taken from Maldeghem *et al.*:[19] $V^2(\tilde{g}_{9/2})=0.87$ for quasiprotons and $V^2(\tilde{s}_{1/2})=0.234$, $V^2(\tilde{d}_{3/2})=0.145$, $V^2(\tilde{d}_{5/2})=0.892$, and $V^2(\tilde{g}_{7/2})=0.674$ for quasineutrons. These occupation probabilities have been obtained using the Nilsson plus pairing model. The corresponding quasiparticle energies are $E(\tilde{d}_{3/2})-E(\tilde{s}_{1/2})=0.32$ MeV, $E(\tilde{d}_{5/2})-E(\tilde{s}_{1/2})=0.81$ MeV, and $E(\tilde{g}_{7/2})-E(\tilde{s}_{1/2})=0.36$ MeV. Since we are considering the low-lying states in a spherical nucleus, the boson core is described by including only the leading term in the SU(5) limit, with the quadrupole boson energy $\hbar\omega_2=1.26$ MeV given by the position of the 2_1^+ state in ^{112}Sn. In this case we can use the reduced boson number[56] $N=2$; this strongly

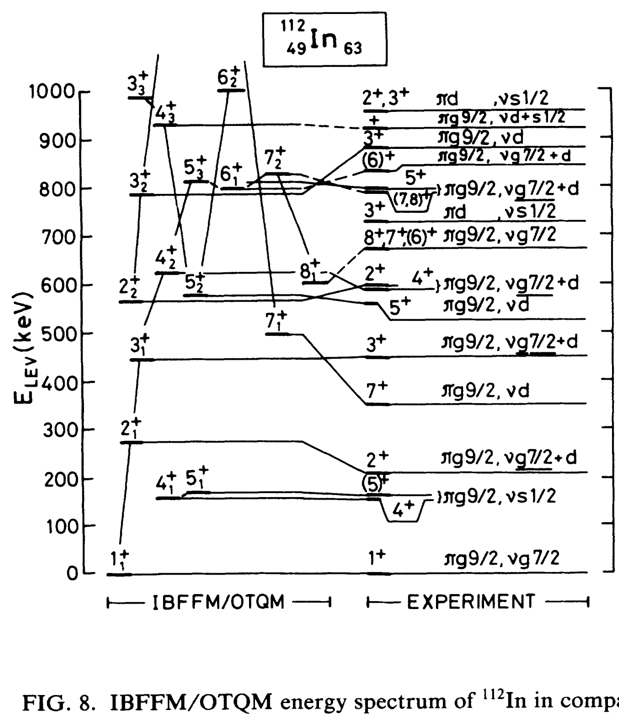

FIG. 8. IBFFM/OTQM energy spectrum of ^{112}In in comparison with experimental data. The solid lines connect the members of the given multiplet.

TABLE VI. Wave functions of low-lying positive-parity states calculated in IBFFM/OTQM. The basis states $|(j_p j_n)j_{pn}, n v I; J\rangle$ are denoted by $(j_p, j_n)j_{pn}, nI$ for a given J. Only amplitudes larger than 5% are listed.

1_1^+		3_2^+	
$(\frac{9}{2},\frac{7}{2})1,00$	−0.806	$(\frac{9}{2},\frac{5}{2})2,12$	−0.399
$(\frac{9}{2},\frac{7}{2})1,12$	−0.259	$(\frac{9}{2},\frac{5}{2})3,00$	−0.747
$(\frac{9}{2},\frac{7}{2})2,12$	0.404	$(\frac{9}{2},\frac{5}{2})4,12$	0.335
$(\frac{9}{2},\frac{7}{2})3,12$	−0.273	$(\frac{9}{2},\frac{5}{2})5,12$	−0.244
2_1^+		3_3^+	
$(\frac{9}{2},\frac{5}{2})2,00$	0.242	$(\frac{9}{2},\frac{3}{2})3,00$	0.787
$(\frac{9}{2},\frac{7}{2})1,12$	−0.381	$(\frac{9}{2},\frac{3}{2})3,12$	0.455
$(\frac{9}{2},\frac{7}{2})2,00$	−0.718		
$(\frac{9}{2},\frac{7}{2})3,12$	0.336		
$(\frac{9}{2},\frac{7}{2})4,12$	−0.271		
2_2^+		4_1^+	
$(\frac{9}{2},\frac{5}{2})2,00$	0.697	$(\frac{9}{2},\frac{1}{2})4,00$	0.580
$(\frac{9}{2},\frac{5}{2})2,12$	0.384	$(\frac{9}{2},\frac{1}{2})4,12$	0.396
$(\frac{9}{2},\frac{5}{2})3,12$	−0.406	$(\frac{9}{2},\frac{3}{2})4,00$	0.488
$(\frac{9}{2},\frac{7}{2})2,00$	0.225	$(\frac{9}{2},\frac{3}{2})4,12$	0.336
		$(\frac{9}{2},\frac{3}{2})5,12$	−0.228
3_1^+		4_2^+	
$(\frac{9}{2},\frac{7}{2})1,12$	−0.258	$(\frac{9}{2},\frac{7}{2})2,12$	−0.250
$(\frac{9}{2},\frac{7}{2})2,12$	−0.315	$(\frac{9}{2},\frac{7}{2})3,12$	−0.302
$(\frac{9}{2},\frac{7}{2})3,00$	−0.747	$(\frac{9}{2},\frac{7}{2})4,00$	−0.750
$(\frac{9}{2},\frac{7}{2})4,12$	0.329	$(\frac{9}{2},\frac{7}{2})5,12$	0.312
$(\frac{9}{2},\frac{7}{2})5,12$	−0.275	$(\frac{9}{2},\frac{7}{2})6,12$	−0.259
4_3^+		6_2^+	
$(\frac{9}{2},\frac{1}{2})4,00$	−0.517	$(\frac{9}{2},\frac{3}{2})5,12$	−0.304
$(\frac{9}{2},\frac{1}{2})4,12$	−0.313	$(\frac{9}{2},\frac{3}{2})6,00$	−0.608
$(\frac{9}{2},\frac{3}{2})4,00$	0.593	$(\frac{9}{2},\frac{3}{2})6,12$	−0.307
$(\frac{9}{2},\frac{3}{2})4,12$	0.331	$(\frac{9}{2},\frac{7}{2})6,00$	0.480
5_1^+		7_1^+	
$(\frac{9}{2},\frac{1}{2})5,00$	−0.609	$(\frac{9}{2},\frac{5}{2})7,00$	−0.681
$(\frac{9}{2},\frac{1}{2})5,12$	−0.433	$(\frac{9}{2},\frac{5}{2})7,12$	−0.554
$(\frac{9}{2},\frac{3}{2})5,00$	0.458	$(\frac{9}{2},\frac{7}{2})7,00$	−0.317
$(\frac{9}{2},\frac{3}{2})5,12$	0.334		
5_2^+		7_2^+	
$(\frac{9}{2},\frac{1}{2})5,00$	−0.460	$(\frac{9}{2},\frac{5}{2})7,00$	0.312
$(\frac{9}{2},\frac{1}{2})5,12$	−0.253	$(\frac{9}{2},\frac{5}{2})7,12$	0.251
$(\frac{9}{2},\frac{3}{2})4,12$	−0.302	$(\frac{9}{2},\frac{7}{2})7,00$	−0.718
$(\frac{9}{2},\frac{3}{2})5,00$	−0.607	$(\frac{9}{2},\frac{7}{2})7,12$	−0.403
$(\frac{9}{2},\frac{3}{2})5,12$	−0.290	$(\frac{9}{2},\frac{7}{2})8,12$	0.237
5_3^+		8_1^+	
$(\frac{9}{2},\frac{7}{2})3,12$	−0.260	$(\frac{9}{2},\frac{7}{2})8,00$	−0.776
$(\frac{9}{2},\frac{7}{2})4,12$	−0.295	$(\frac{9}{2},\frac{7}{2})8,12$	−0.552
$(\frac{9}{2},\frac{7}{2})5,00$	−0.787		
$(\frac{9}{2},\frac{7}{2})6,12$	0.303		
6_1^+			
$(\frac{9}{2},\frac{3}{2})6,00$	0.471		
$(\frac{9}{2},\frac{3}{2})6,12$	0.263		
$(\frac{9}{2},\frac{7}{2})6,00$	0.645		
$(\frac{9}{2},\frac{7}{2})6,12$	0.233		
$(\frac{9}{2},\frac{7}{2})7,12$	−0.226		

TABLE VII. Magnetic dipole (μ in μ_N) and electric quadrupole (Q in eb) moments of some ^{112}In states.

Electromagnetic moments	^{112}In states: 1_1^+ ground 14.4 min	4_1^+ 20.9 min	7_1^+ 0.69 μs
μ_{exp}	+2.82(3)[a]	+5.277(5)[b]	+4.056(36)[a,e]
μ_{emp}	+3.07	+5.98	+4.44
$\mu_{theor,IBFFM}$	+2.82	+5.29	+4.54
μ_{theor}	+2.84[c]		
Q_{exp}	+0.093[a]	+0.714(10)[b]	0.75(15)[d,e]
Q_{emp}	+0.17	+0.75[b]	+1.11
$Q_{theor,IBFFM}$	+0.14	+0.67	+0.84
Q_{theor}	+0.102[c]		

[a]Reference 61.
[b]Reference 60.
[c]Reference 19.
[d]Reference 62.
[e]Formerly 6^+ spin and parity was assigned to this state.

reduces the scope of computations, without sizeable effect on the properties of the low-lying states which are being investigated. The boson fermion interaction strengths are $\Gamma_0^p = 1.9$ MeV (fitted to the energy spectrum of ^{111}In) and $\Gamma_0^n = 0.8$ MeV (adjusted to the lifetime of 7_1^+ state). The strengths of the exchange interaction were $\Lambda_0^p = 0$ (taking into account that the boson/phonon consists mainly of neutron excitations) and $\Lambda_0^n = 0.8$ MeV (fitted to the γ branching ratios of ^{112}In). The strengths of the residual force, adjusted to the energy spectrum of ^{112}In, are $v_D = -0.4$ MeV, and $v_S = -0.1$ MeV, including the radial integrals.

The calculated energy spectrum of positive parity states is presented in Fig. 8, in comparison with the experimental data up to ~1 MeV. As seen, the calculated low-lying levels have the corresponding experimental counterparts. The level energies are generally in good agreement with the experimental ones and also with the results of the parabolic rule calculations.

In Table VI the calculated wave functions of the low-lying states are displayed. It is seen that IBFFM/OTQM calculation for most low-lying states preserves the approximate classification of the parabolic rule: the $1_1, 2_1, 3_1, 4_2, 5_3, 6_1, 7_2, 8_1$ states are dominated by components with $\pi\tilde{g}_{9/2}, \nu\tilde{g}_{7/2}$ quasiparticles, the $2_2, 3_2, 4_4, 5_4, 6_3, 7_1$ by components with $\pi\tilde{g}_{9/2}, \nu\tilde{d}_{5/2}$, and $3_3, 4_3, 5_2, 6_2$ by components with $\pi\tilde{g}_{9/2}, \nu\tilde{d}_{3/2}$ quasiparticles. (See also Figs. 6–8.) According to the parabolic rule calculation, the $4_1, 5_1$ and $4_3, 5_2$ states belong to the $\pi\tilde{g}_{9/2}, \nu\tilde{s}_{1/2}$ and $\pi\tilde{g}_{9/2}, \nu\tilde{d}_{3/2}$ multiplets, respectively. However, in the calculated wave function these two-quasiparticle configurations strongly mix. The pronounced components in the wave functions of the 4_1 and 4_3 states are

TABLE VIII. Transitions within low-lying ^{112}In states.

States				E_γ	$I_\gamma^{\rm Rel}/E_\gamma^3$		Type		
E_i (keV)	J_i	E_f (keV)	J_f	(keV)	Exp.	IBFFM	Experiment	Kohno *et al.* (Ref. 9)	IBFFM
206.72	2_1^+	0.0	1_1^+	206.75			$M1$		$M1+0.084\%$ $E2$
456.45	3_1^+	206.72	2_1^+	249.68			$M1$		$M1+0.079\%$ $E2$
562.79	5_2^+	162.90	$(5_1)^+$	399.88	52(3)	10	$M1,E2$		$M1+0.004\%$ $E2$
		156.61	4_1^+	406.18	100	100	$M1,E2$		$M1+0.61\%$ $E2$
592.10	4_2^+	456.45	3_1^+	135.64	100	100	$M1$	$M1+[0.01(20)]\%$ $E2$	$M1+0.022\%$ $E2$
		162.90	$(5_1)^+$	429.17	0.3(1)	3			$M1+0.018\%$ $E2$
594.87	2_2^+	456.45	3_1^+	138.37	69(8)	16			$M1+0.003\%$ $E2$
		206.72	2_1^+	388.20	100	100	$M1,E2$	$M1+[0.25(50)]\%$ $E2$	$M1+0.051\%$ $E2$
		0.0	1_1^+	594.85	83(4)	85	$M1,(E2)$	$M1+[1.0(6)]\%$ $E2$	$M+0.97\%$ $E2$
790.28	$(7_2^+,8)^+$	670.24	$8_1^+,7^+(6)^+$	120.01	100	100			$M1+0.024\%$ $E2$
		350.81	7_1^+	439.49	20(4)	11	$M1,E2$		$M1+0.32\%$ $E2$
795.27	5_3^+	592.10	4_2^+	203.17			$M1$	$M1+[0.01(22)]\%$ $E2$	$M1+0.054\%$ $E2$
833.10	6_1^+	562.79	5_2^+	270.22	43(10)	37			$M1+0.27\%$ $E2$
		350.81	7_1^+	482.39	100	100	$M1,E2$		$M1+0.10\%$ $E2$
		162.90	$(5_1)^+$	670.19	4(1)	14	$M1$		$M1+4.9\%$ $E2$
883.79	3_2^+	594.87	2_2^+	288.92	100	100	$M1$	$M1+[0.25(30)]\%$ $E2$	$M1+0.13\%$ $E2$
		592.10	4_2^+	291.5	4(2)	0.6			$M1+0.32\%$ $E2$
		456.43	3_1^+	427.39	3(1)	0.4			$M1+1.1\%$ $E2$
		156.61	4_1^+	727.25	5(1)	6			$M+0.003\%$ $E2$

$$|4_1\rangle=0.58\,|(\pi\tilde{g}_{9/2},\nu\tilde{s}_{1/2})4,00;4\rangle+0.40\,|(\pi\tilde{g}_{9/2},\nu\tilde{s}_{1/2})4,12;4\rangle$$
$$+0.49\,|(\pi\tilde{g}_{9/2},\nu\tilde{d}_{3/2})4,00;4\rangle+0.34\,|(\pi\tilde{g}_{9/2},\nu\tilde{d}_{3/2})4,12;4\rangle\ ,$$
$$|4_3\rangle=-0.52\,|(\pi\tilde{g}_{9/2},\nu\tilde{s}_{1/2})4,00;4\rangle-0.31\,|(\pi\tilde{g}_{9/2},\nu\tilde{s}_{1/2})4,12;4\rangle$$
$$+0.59\,|(\pi\tilde{g}_{9/2},\nu\tilde{d}_{3/2})4,00;4\rangle+0.33\,|(\pi\tilde{g}_{9/2},\nu\tilde{d}_{3/2})4,12;4\rangle\ ,$$

and can be approximately presented as

$$|4_1\rangle\simeq\frac{1}{\sqrt{2}}(\,|4_3^{(0)}\rangle+|4_1^{(0)}\rangle)\ ,$$
$$|4_3\rangle\simeq\frac{1}{\sqrt{2}}(\,|4_3^{(0)}\rangle-|4_1^{(0)}\rangle)\ ,$$

where $|4_1^{(0)}\rangle$ and $|4_3^{(0)}\rangle$ denote the wave functions associated with $(\pi\tilde{g}_{9/2},\nu\tilde{s}_{1/2})$ and $(\pi\tilde{g}_{9/2},\nu\tilde{d}_{3/2})$ two-quasiparticle multiplets, respectively.

An interesting result of the OTQM calculations is that the level sequence of the 4^+ and 5^+ members of the $\pi\tilde{g}_{9/2}\nu\tilde{s}_{1/2}$ multiplet has been correctly reproduced. The purity of these states is remarkably less than in the case of ^{114}In (53% and 58% at ^{112}In and 59% and 70% at ^{114}In,[58] respectively).

Employing the wave functions from diagonalization, we have calculated the electromagnetic properties. For effective proton and neutron charges and for gyromagnetic ratios the standard values have been used: $e_{\rm p}^{\rm s.p.}=1.5$, $e_{\rm n}^{\rm s.p.}=0.5$, $g_l^p=1$, $g_l^n=0$, $g_s^p=0.5g_s^p$ (free), $g_s^n=0.5g_s^n$ (free), $g_R=Z/A$. The boson charge $e_{\rm vib}=2.5$ was fitted (in conjunction with Γ_0^n) to the measured half-life of the 7_1^+ level, $\tau(7_1^+)=0.69$ μs.

In Table VII the calculated $E2$ and $M1$ static moments are presented for the low-lying levels, in comparison with the experimental data. The empirical values, obtained from the corresponding experimental moments of the neighboring odd-even In, Sn, and Cd nuclei on the basis of simple additivity relations[59] and the theoretical results of Van Maldeghem *et al.*[19] are also given.

The sign of the $\mu_{\rm exp}$ and $Q_{\rm exp}$ values was properly reproduced both in the OTQM and additivity relation calculations. The $\mu_{\rm exp}$, $\mu_{\rm emp}$, and $\mu_{\rm theor,IBFFM}$ values agree within $\sim$13%. The deviations among the $Q_{\rm exp}$, $Q_{\rm emp}$, and $Q_{\rm theor,IBFFM}$ values are greater, but even these values agree within $\sim$70%. The IBFFM calculations show that the contribution of the collective electromagnetic operator to the magnetic moments is relatively small. This can explain why the simple additivity relation predicts the moments correctly.

In Table VIII we present the reduced transition probabilities and mixing ratios of $M1+E2$ transitions between the low-lying states. As seen, the IBFFM calculation reproduces the experimental data reasonably well. The relative γ-ray intensities of crossover $E2$ transitions from the 3_1 and 4_2 states are also correctly reproduced [1% and 3% compared to 3% (2) and 6% (4) experimental values].

The ordering of experimental and theoretical levels to each other was made on the basis of energy, spin, parity, configuration, and decay data. In some cases the composition of the wave function, the configuration determined from nucleon transfer reactions, as well as the theoretical and experimental γ-decay properties enabled probable identification, although the J^{π} values were not known unambiguously. For example, at the 833.10 keV $J^{\pi}=(6)^{+}$, 790.28 keV $J^{\pi}=7^{+},8^{+}$, and 923 keV positive parity states, which have been identified with the 6_1^+, 7_2^+, and 4_3^+ IBFFM states, respectively.

ACKNOWLEDGMENTS

The assistance in experiments of the Debrecen and Jyväskylä cyclotron staffs, as well as the members of the Debrecen cryogenic laboratory is recognized. We are indebted also to Dr. J. Gulyás, Dr. S. Mészáros and Dr. A. Valek for their help in the measurements and Dr. T. Vertse for his help in the Hauser-Feshbach calculations.

---

*Present address: University of Joensuu, Department of Physics, SF-80101 Joensuu, Finland.

[1]S. A. Hjorth and L. H. Allen, Ark. Fys. **33**, 121 (1967).

[2]H. F. Brinckmann, W. D. Fromm, C. Heiser, and H. Rotter, Zentralinstitut für Kernforschung, Rossendorf bei Dresden Report No. ZfK-243, 1972, p. 41.

[3]W. D. Fromm, H. F. Brinckmann, U. Hagemann, C. Heiser, and H. Rotter, Zentralinstitut für Kernforschung, Rossendorf bei Dresden Report No. ZfK-262, 1973, p. 59.

[4]M. Eibert, A. K. Gaigalas, and N. I. Greenberg, J. Phys. B **2**, L203 (1976); M. Eibert, Ph.D. thesis, State University of New York, Binghamton, 1977.

[5]L. E. Samuelson, R. E. Anderson, R. A. Emigh, and P. A. Smith, Colorado State University Report No. C00-535-766, 1978, p. 25; L. E. Samuelson, R. A. Emigh, and R. E. Anderson, Bull. Amer. Phys. Soc. **23**, 962 (1978).

[6]R. A. Emigh, R. E. Anderson, and L. E. Samuelson, Colorado State University Report No. C00-535-766, 1978, p. 64.

[7]R. A. Emigh, R. E. Anderson, L. E. Samuelson, and C. A. Fields, Colorado State University Report No. C00-535-767, 1979, p. 82.

[8]M. Adachi, A. Muroi, T. Matsuzaki, and H. Taketani, Z. Phys. A **295**, 251 (1980).

[9]T. Kohno, M. Adachi, and H. Taketani, Nucl. Phys. **A398**, 493 (1983).

[10]L. K. Peker, Nucl. Data Sheets **29**, 587 (1980).

[11]E. Bleuler, J. W. Blue, S. A. Chowdary, A. C. Johnson, and D. J. Tendam, Phys. Rev. **90**, 464 (1953).

[12]T. Kozlowski, Z. Moroz, E. Rurarz, and J. Wojtkowska, Acta Phys. Pol. **33**, 409 (1968).

[13]M. Ionescu-Bujor, E. A. Ivanov, A. Iordachescu, D. Plostinaru, and G. Pascovici, Phys. Lett. **64B**, 36 (1976).

[14]M. Ionescu-Bujor, E. A. Ivanov, A. Iordachescu, D. Plostinaru, and G. Pascovici, Nucl. Phys. **A272**, 1 (1976).

[15]M. Ionescu-Bujor, E. A. Ivanov, A. Iordachescu, D. Plostinaru, and Gh. Pascovici, Hyperfine Interact. **2**, 324 (1976).

[16]T. B. Ryves, Ma Hongchang, S. Judge, and P. Kolkowski, J. Phys. G **9**, 1549 (1983).

[17]K. A. Baskova, Yu. V. Krivonogov, B. M. Makuni, E. A. Skakun, T. V. Chugai, and L. Ya. Shavtvalov, Izv. A. N. SSSR, Ser. Fiz. **48**, 38 (1984).

[18]J.-Z. Ruan and Y. Yoshizawa, Nucl. Phys. **36**, 431 (1962).

[19]J. Van Maldeghem, K. Heyde, and J. Sau, Phys. Rev. C **32**, 1067 (1985).

[20]V. Paar, in *In-Beam Nuclear Spectroscopy,* edited by Zs. Dombrádi and T. Fényes (Akad. Kiadó, Budapest, 1984), Vol. 2, p. 675.

[21]A. H. Wapstra and G. Audi, Nucl. Phys. A **432**, 1 (1985).

[22]R. Julin, J. Kantele, J. Kumpulainen, M. Luontama, V. Nieminen, A. Passoja, W. Trzaska, and E. Verho, University of Jyväskylä, JYFL Ann. Rep. 2.1, 1985.

[23]Z. Árvay, T. Fényes, K. Füle, T. Kibédi, S. László, Z. Máté, Gy. Mórik, D. Novák, and F. Tárkányi, Nucl. Instrum. Methods **178**, 85 (1980); T. Kibédi, Z. Gácsi, A. Krasznahorkay, and S. Nagy, ATOMKI Annual Report, Debrecen, 1986, p. 55; T. Kibédi, Z. Gácsi, and A. Krasznahorkay, ATOMKI Annual Report, Debrecen, 1987.

[24]G. Székely, Comput. Phys. Commun. **34**, 313 (1985).

[25]R. S. Hager and E. C. Seltzer, Nucl. Data Tables A **4**, 1 (1968).

[26]J. Lyttkens, K. Nilson, and L. P. Ekström, Nucl. Data Sheets **33**, 1 (1981).

[27]J. Blachot, Nucl. Data Sheets **41**, 111 (1984).

[28]B. P. Casserberg and E. A. Phillips, private communication in Ref. 10.

[29]E. Sheldon and V. C. Rogers, Comp. Phys. Commun. **6**, 99 (1973).

[30]D. Wilmore and P. E. Hodgson, Nucl. Phys. **55**, 673 (1964).

[31]F. G. Perey, Phys. Rev. **131**, 745 (1963).

[32]B. Gyarmati, T. Vertse, L. Zolnai, A. I. Barishnikov, A. F. Gurbich, N. N. Titarenko, and E. L. Yadrovsky, J. Phys. G **5**, 1225 (1979).

[33]M. Conjeaud, S. Harar, and E. Thuriere, Nucl. Phys. **A129**, 10 (1969).

[34]R. G. Markham and H. W. Fulbright, Phys. Rev. C **9**, 1633 (1974).

[35]E. Hagn and E. Zech, Phys. Rev. C **24**, 2222 (1981).

[36]G. Ulm, J. Eberz, G. Huber, H. Lochmann, R. Menges, R. Kirchner, O. Klepper, T. Kühl, P. O. Larsson, D. Marx, D. Murnick, and D. Schardt, Z. Phys. A **321**, 395 (1985).

[37]B. I. Atalay and L. W. Chiao-Yap, Phys. Rev. C **5**, 369 (1972).

[38]J. W. Smits and R. H. Siemssen, Nucl. Phys. **A261**, 385 (1976).

[39]P. E. Cavanagh, C. F. Coleman, A. G. Hardacre, G. A. Gard, and J. F. Turner, Nucl. Phys. A **141**, 97 (1970).

[40]D. G. Fleming, Can. J. Phys. **60**, 428 (1982).

[41]T. Borello, E. Frota-Pessoa, C. Q. Orsini, O. Deitzsch, and E. W. Hamburger, Rev. Bras. Fis. **2**, 157 (1972).

[42]R. A. Sorensen, Nucl. Phys. **25**, 674 (1961).

[43]V. Paar, Nucl. Phys. **A331**, 16 (1979).

[44]A. Calboreanu and S. Mancas, Nucl. Phys. **A266**, 72 (1976).

[45]R. A. Emigh, C. A. Fields, M. L. Gartner, L. E. Samuelson, and P. A. Smith, Z. Phys. A **308**, 165 (1982).

[46]B. Rosner, Phys. Rev. **136B**, 664 (1964).

[47]S. Harar and R. N. Horoshko, Nucl. Phys. **A183**, 161 (1972).

[48]A. Krasznahorkay, T. Fényes, J. Timár, T. Kibédi, A. Passoja, R. Julin, and J. Kumpulainen, Nucl. Phys. **A473**, 471 (1987).

[49]J. Timár, T. Fényes, T. Kibédi, A. Passoja, M. Luontama, W. Trzaska, and V. Paar, Nucl. Phys. **A455**, 477 (1986).

[50]P. H. Stelson and L. Grodzins, Nucl. Data A **1**, 21 (1965).

[51]S. Brant, V. Paar, and D. Vretenar, Z. Phys. A **319**, 355 (1984); T. Hübsch, V. Paar, and D. Vretenar, Phys. Lett. **151B**, 320 (1985); V. Lopac, S. Brant, V. Paar, O. W. B. Schult, H. Seyfarth, and A. B. Balantekin, Z. Phys. A **323**, 491 (1986); S. Brant, V. Paar, D. Vretenar, G. Alaga, H. Seyfarth, O. Schult, and M. Bogdanovic, Phys. Lett. B **195**, 111 (1987).
[52]A. Arima and F. Iachello, Phys. Rev. Lett. **35**, 1069 (1975).
[53]F. Iachello and O. Scholten, Phys. Rev. Lett. **43**, 679 (1979).
[54]D. Janssen, R. V. Jolos, and F. Dönau, Nucl. Phys. **A224**, 93 (1974).
[55]V. Paar, S. Brant, L. F. Canto, G. Leander, and M. Vouk, Nucl. Phys. **A378**, 41 (1982).
[56]A. B. Balantekin and V. Paar, Phys. Lett. **169B**, 9 (1986).
[57]S. Brant, V. Paar, and D. Vretenar (unpublished).
[58]T. Fényes, Zs. Dombrádi, A. Krasznahorkay, T. Kibédi, and J. Timár, ATOMKI, Debrecen, Preprint A/21, 1987.
[59]R. J. Blin-Stoyle, Rev. Mod. Phys. **28**, 75 (1956); P. J. Brussaard and P. W. M. Glaudemans, *Shell-Model Applications in Nuclear Spectroscopy* (North-Holland, Amsterdam, 1977), p. 256.
[60]J. Eberz, U. Dinger, G. Huber, H. Lochmann, R. Menges, R. Neugart, R. Kirchner, O. Klepper, T. Kühl, D. Marx, G. Ulm, K. Wendt, and the ISOLDE Collaboration, Nucl. Phys. **A464**, 9 (1987).
[61]C. M. Lederer and V. S. Shirley, *Table of Isotopes* (Wiley, New York, 1978), Appendix VII.
[62]M. Ionescu-Bujor, A. Iordachescu, E. A. Ivanov, and D. Plostinaru, Hyperfine Interact. **11**, 71 (1981).